FAM83H Mutations in Families with Autosomal-Dominant Hypocalcified Amelogenesis Imperfecta

Jung-Wook Kim,[1,2,*] Sook-Kyung Lee,[1] Zang Hee Lee,[1] Joo-Cheol Park,[1] Kyung-Eun Lee,[1] Myoung-Hwa Lee,[4] Jong-Tae Park,[4] Byoung-Moo Seo,[3] Jan C.-C. Hu,[5] and James P. Simmer[5]

Amelogenesis imperfecta (AI) is a collection of diverse inherited disorders featuring dental-enamel defects in the absence of significant nondental symptoms. AI phenotypes vary and are categorized as hypoplastic, hypocalcified, and hypomaturation types. Phenotypic specificity to enamel has focused research on genes encoding enamel-matrix proteins. We studied two families with autosomal-dominant hypocalcified AI and have identified nonsense mutations (R325X and Q398X) in the *FAM83H* gene on chromosome 8q24.3. The mutations perfectly cosegregate with the disease phenotype and demonstrate that FAM83H is required for proper dental-enamel calcification.

Dental enamel is the most highly mineralized tissue in the human body. Mature enamel contains less than 1% organic material. It is acellular and contains no collagen. Enamel forms in an extracellular space lined by ameloblasts, tightly connected epithelial cells that control both the ionic and the organic contents of the enamel extracellular space.[1] The mineral in enamel is mainly calcium hydroxyapatite, but the dimensions of its crystallites are unlike any observed outside of amelogenesis. The final crystals are only about 25 nm thick and 65 nm wide but are believed to extend, uninterrupted, from the dentino-enamel junction to the surface of the tooth, a distance of up to 2 mm.[2] These crystallites grow parallel to each other in bundles called rods, with about 10,000 crystallites per rod.[3] Enamel crystallites extend at a mineralization front located at the secretory portion of the ameloblast distal membrane. Proteins secreted at this site act in concert to lengthen the crystals. These proteins are amelogenin (AMELX),[4] enamelin (ENAM),[5] ameloblastin (AMBN),[6] and the protease enamelysin (MMP20).[7] *Amelx*, *Enam*, and *Ambn* null mice produce either a thin or a nonexistent enamel layer.[8–10] *Mmp20* null mice produce an enamel layer about half as thick as normal.[11] Defects in human *AMELX*, *ENAM*, and *MMP20* cause X-linked hypoplastic/hypomaturation forms (MIM 301200), autosomal-dominant and -recessive hypoplastic forms (MIM 608563), and autosomal-recessive pigmented hypomaturation forms (MIM 204700) of AI, respectively.[12–15] Kallikrein 4 (KLK4) is a serine protease expressed at a later stage of enamel formation,[16] and it causes autosomal-recessive pigmented hypomaturation AI (MIM 204700).[17] It is therefore well established that defects in the genes encoding enamel extracellular-matrix proteins cause AI. It is also established that only about ¼ of all AI cases are caused by these genes.[18]

AI is the collective designation given to inherited enamel defects that occur in the absence of significant non-dental phenotypes. Allele frequency differences cause the prevalence of AI to vary geographically; it is 1:700 in Sweden and 1:14,000 in the United States. Hypocalcified AI is the most common type of AI in the United States.[19] AI is a heterogeneous disorder that can be caused by mutations in a variety of genes. The defects include thin (hypoplastic) enamel associated with defective matrix synthesis; soft, rough (hypocalcified) enamel from a failure in calcification; and soft, stained (hypomatured) enamel of normal thickness, a defect associated with a failure to remove enamel proteins and allow the crystals to fill the space between crystallites. On the basis of the phenotype and pattern of inheritance, 14 mostly distinct forms are recognized.[20] Because the phenotype is limited to the dentition, the genes encoding enamel proteins were long suspected of causing AI, and indeed all but ameloblastin are proven to be part of its etiology.

The proteins in the enamel matrix of developing teeth have been extensively characterized.[21,22] The enamel proteome is composed predominantly of amelogenin and, to a lesser extent, enamelin and ameloblastin cleavage products.[23,24] The likelihood that many more genes that encode critical matrix constituents will be identified is low. Recently, however, a novel component of the maturation-stage basal lamina, amelotin (AMTN), was discovered.[25] *AMTN* is now a candidate gene for hypomaturation forms of AI, but mutation analyses of *AMTN* have not yet turned up any disease-causing mutations.

More often than not, mutation analyses of kindreds with AI do not identify a disease-causing mutation, that is, one that causes a predictable loss of protein function and also correlates with the disease phenotype.[18] Sometimes, linkage to known candidate genes can be excluded,[26] and,

[1]Department of Cell and Developmental Biology and Dental Research Institute, [2]Department of Pediatric Dentistry & Dental Research Institute, [3]Department of Oral and Maxillofacial Surgery and Dental Research Institute, School of Dentistry, Seoul National University, 275-1 Yongon-dong, Chongno-gu, Seoul 110-768, Korea; [4]Department of Oral Histology, College of Dentistry, Chosun University, 375 Seosug-dong, Dong-gu, Gwang-Ju, 501-759, Korea; [5]Department of Biologic and Materials Sciences, University of Michigan Dental Research Lab, 1210 Eisenhower Place, Ann Arbor, MI 48108, USA
*Correspondence: pedoman@snu.ac.kr
DOI 10.1016/j.ajhg.2007.09.020.

Table 1. Primer Pairs Used to Amplify and Sequence the *FAM83H* Gene

Amplicon	Forward	Reverse
1	5′-CAGGAGGCAGGAGCGAC-3′	5′-GGTAGCCCAAGTGGGACC-3′
2	5′-TCCACAGTGTGTCCATGCTC-3′	5′-GCTCATGCATCTCCTCCAC-3′
3	5′-GTGATCCAGACACCTCCCG-3′	5′-CCTGGTGTGGAAAGGGG-3′
4	5′-AGACCTCACATCCCTGCG-3′	5′-CTTGAAGGCGTCCATCTCC-3′
5	5′-ACTTCCTGTCGGCCTTCC-3′	5′-GTAGGAGGCCAAACGCC-3′
6	5′-GGACTACGTGCCGTCCAG-3′	5′-AGCAGCTGCACCTTCTCAG-3′
7	5′-AGCAGGACTCATTCCGCTC-3′	5′-GACTCATTATGGAGCACCTGG-3′
8	5′-AGCTGCTCGACACACTGG-3′	5′-GCCCAGTGACAGACGCC-3′
9	5′-AAGGCTCCTTGCGTCTTAGG-3′	5′-CTGCTGGCCTCCTCTTTC-3′
10	5′-TCCGCTCGGACAGCTTG-3′	5′-AGCCCAGACCGCTCAAC-3′
11	5′-AGCACCTTCATCTCTGCACC-3′	5′-AGCGAGCAGGAGAATCCAAG-3′
12	5′-CTCAGGGCCTCCTGTTCTC-3′	5′-CCCATACCTGTCAAGGATAAGC-3′
13	5′-ATGGTCCAGACAACCTGTGG-3′	5′-GGAACTGCTGCCTTTGTTTG-3′
14	5′-TGTAGAAAGCCCCCACTGTT-3′	5′-GTCCACAGGGGAAATCTGG-3′

Table 2. Two-Point LOD Scores of the Locus Associated with ADHCAI Family 1

Marker	Physical Position	Θ 0.0	0.05	0.10	0.15	0.20	0.30	0.40
D8S347	129,409,639	−∞	−1.62	−0.44	0.10	0.37	0.51	0.34
D8S378	134,105,713	−∞	−0.50	−0.22	−0.08	0.00	0.07	0.07
D8S1837	139,301,331	−∞	1.48	1.53	1.45	1.31	0.93	0.46
D8S1050	139,724,990	2.46	2.23	1.99	1.75	1.50	0.99	0.45
D8S1024	141,497,876	2.67	2.36	2.12	1.90	1.68	1.14	0.52
D8S1704	141,720,546	4.64	4.29	3.90	3.47	3.01	2.00	0.91
D8S1744	143,101,154	3.78	3.45	3.11	2.76	2.39	1.62	0.80
D8S161	143,444,797	5.55	5.04	4.52	3.98	3.41	2.21	0.97
D8S1836	143,747,505	5.86	5.36	4.84	4.29	3.73	2.52	1.21
D8S315	144,218,310	5.83	5.33	4.81	4.27	3.71	2.50	1.21
D8S373	144,296,507	3.41	3.11	2.80	2.48	2.14	1.45	0.70
D8S2334	146,101,309	3.40	3.11	2.81	2.49	2.16	1.47	0.73
D8S1926	146,114,938	5.70	5.21	4.70	4.18	3.62	2.45	1.17

Physical position is based on Build 36.2 of the GenBank human reference sequence.

rarely, linkage is established to a particular chromosomal segment. Recently, a 2.1 Mb region on chromosome 8q24.3 was mapped as a previously unreported disease locus for a Brazilian family with autosomal-dominant hypocalcified AI (ADHCAI), but the linkage area contained no apparent candidate genes, and the causative gene was not identified.[27] Here we report that we have identified a gene in this region that causes ADHCAI. To our knowledge, it is the first AI gene that has been identified through a genome-wide search and encodes an intracellular protein that is ubiquitously expressed rather than being specific for tooth formation. The gene has no previously known connection to amelogenesis.

The study protocol and patient consents were independently reviewed and approved by the Institution Review Board at the Seoul National University Dental Hospital. Informed-consent procedure was conducted according to the Declaration of Helsinki.

Genomic DNA was obtained by a conventional salting-out method. The purity and concentration of the DNA was quantitated by spectrophotometry, as measured by the OD_{260}/OD_{280} ratio. DNA concentration was adjusted to 10 ng/μl. Thirteen polymorphic markers were genotyped for 25 individuals (14 affected and 11 unaffected) in a Korean ADHCAI family 1 by use of fluorescene-labeled primers. Genotyping was performed at the National Instrumentation Center for Environmental Management (NICEM, Seoul National University, Seoul, Korea). Analysis of linkage was performed via *FastLink v4.1* in *easyLINKAGE Plus v5.02*, with a stringent autosomal-dominant model that specified a penetrance of 1 and disease-allele frequency of 0.001 as input values.[28]

Mutations were sought in 42 genes, including *FAM83H* (family with sequence similarity 83 member H) in the 2.1 Mb linkage region, by direct DNA sequencing of the proband. PCR primers were generated with the help of the *ExonPrimer* and *Primer3* on the web. PCR primers for exons and exon/intron boundaries of *FAM83H* are listed in Table 1. PCR amplifications were performed with the HiPi DNA polymerase premix (ElpisBio, Korea). PCR-amplification products were purified with the PCR Purification Kit and protocol (ElpisBio, Korea). DNA sequencing was performed at the DNA-sequencing center (Macrogen, Korea). Both identified mutation sites were analyzed in all family members and in genomic DNA from 200 unrelated Korean normal control chromosomes by direct DNA sequencing as described above.

To detect mRNA in the tooth samples we performed in situ hybridization. A database search identified the mouse homolog of *FAM83H*: *AA409316*. Based on the mRNA sequence (NM_134087.1), primers were designed to amplify a 539 bp probe (forward primer: 5′-TGCGCTCATCACTCATCTTT-3′; reverse primer: 5′-ATAAGGCAGCTGGTGTGTCC-3′). The amplified product was cloned into the pCR2.1-TOPO vector (Invitrogen, USA) and subcloned into the pBluescript II SK(+) vector (Stratagene, USA). The pBluescript II SK(+) construct was restricted with BamHI and DIG-labeled with the DIG RNA Labeling kit. Mandible specimens from 3-week-old mice were hybridized with the labeled probe according to the manufacturer's protocol. Each section was counterstained with methyl green.

For investigation of the expression of *FAM83H* in the tooth follicle, RT-PCR was performed with RNA from a human tooth follicle, human pulp tissue, and tissues from a newborn mouse. Primers for the mouse tissues were the same as those used for in situ hybridization. Primers for the amplification (amplicon 10) of *FAM83H* were used for human tissues. *GAPDH* was used as an internal control.

Linkage analysis confirmed the disease locus to be within the chromosome 8q24.3 region, between *D8S1837* and the telomere (Table 2, Figure 1). There are 91 genes in the overlapping region. We performed mutation analyses for 42 of these genes and identified a nonsense mutation in exon 5 of the *FAM83H* (Figure 2). On the basis of the GenBank reference sequences NC_000008.9 and NM_198488.2, the mutation is designated 973C→T; R325X. This mutation perfectly cosegregates with the disease phenotype in this

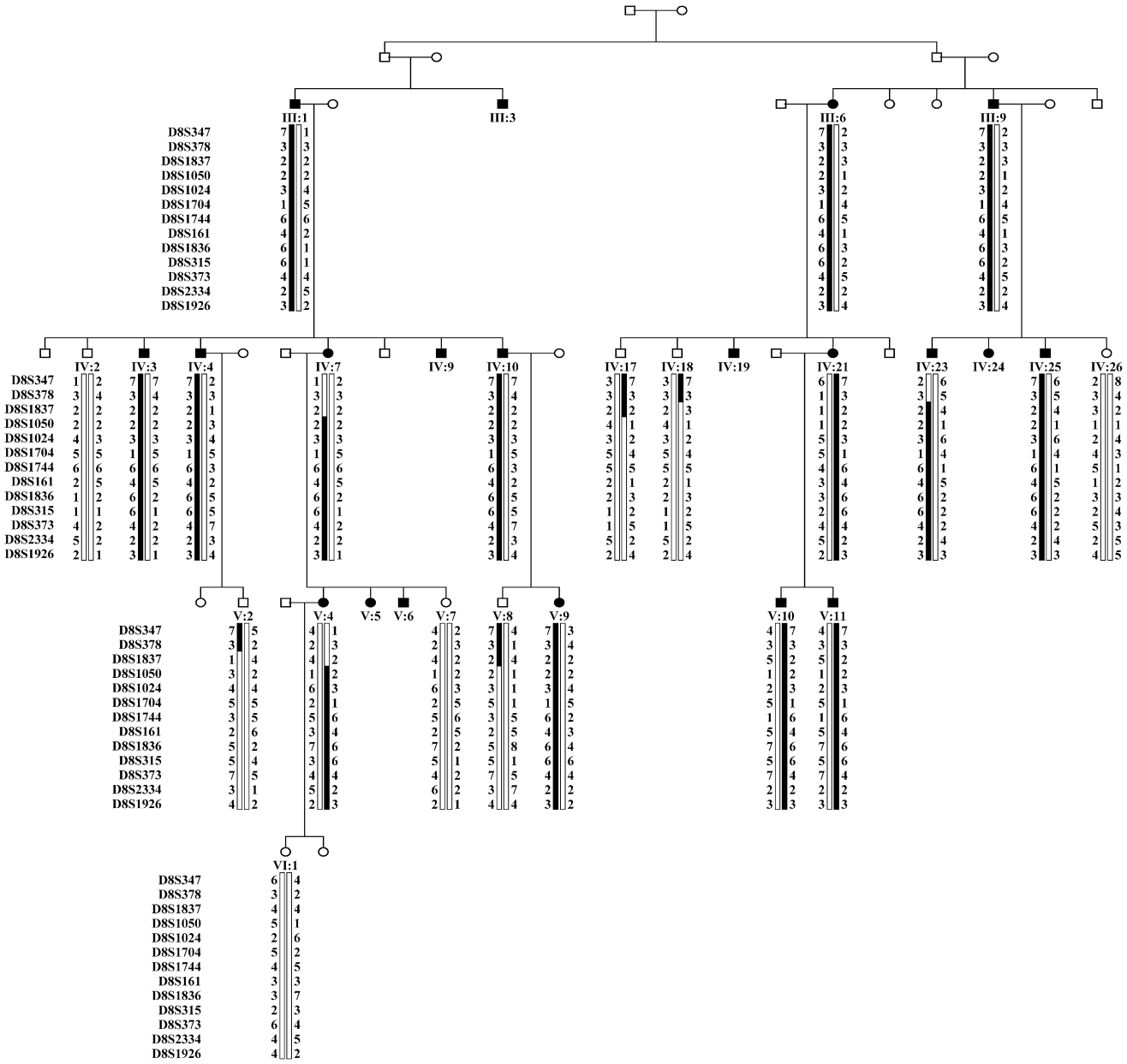

Figure 1. Pedigree and Haplotype of the ADHCAI Family 1

Affected individuals are indicated by black symbols including the proband (V:11). Squares represent males, and circles represent females. Bars shown below each individual indicate the genotypes of the microsatellite markers. The black bar represents the marker haplotype that segregates with the affected status. Microsatellite markers are shown in their chromosomal order.

family. Subsequently, we identified a spontaneous nonsense mutation (1192C→T; Q398X) in the same gene in another Korean ADHCAI family. In both families, the disease-causing mutation was a premature translation-termination codon in the last exon. Both mutations were absent in genomic DNA analyzed from 200 unrelated Korean normal control chromosomes. In addition to the perfect correlation with the disease phenotype among 25 individuals, the two *FAM83H* mutations we identified would have significantly truncated the expressed protein and certainly affected its function. The wild-type FAM83H protein has 1179 amino acids, a calculated molecular mass of 127-kDa, and an isoelectric point of 6.6 (Figure 2C). The R325X and Q398X mutant proteins are 855 and 782 amino acids shorter than the wild-type protein, respectively. We have also confirmed by in situ hybridization and RT-PCR that *FAM83H* is expressed by ameloblasts (Figure 3). The data strongly support the hypothesis that the identified *FAM83H* mutations caused ADHCAI in these families.

The dental enamel in affected members of these kindreds was of normal thickness in unerupted or newly erupted teeth, but was cheesy soft and lost soon after eruption (Figure 2A). Clinically, the teeth were extremely sensitive to thermal irritation. Because of rapid attrition and painful

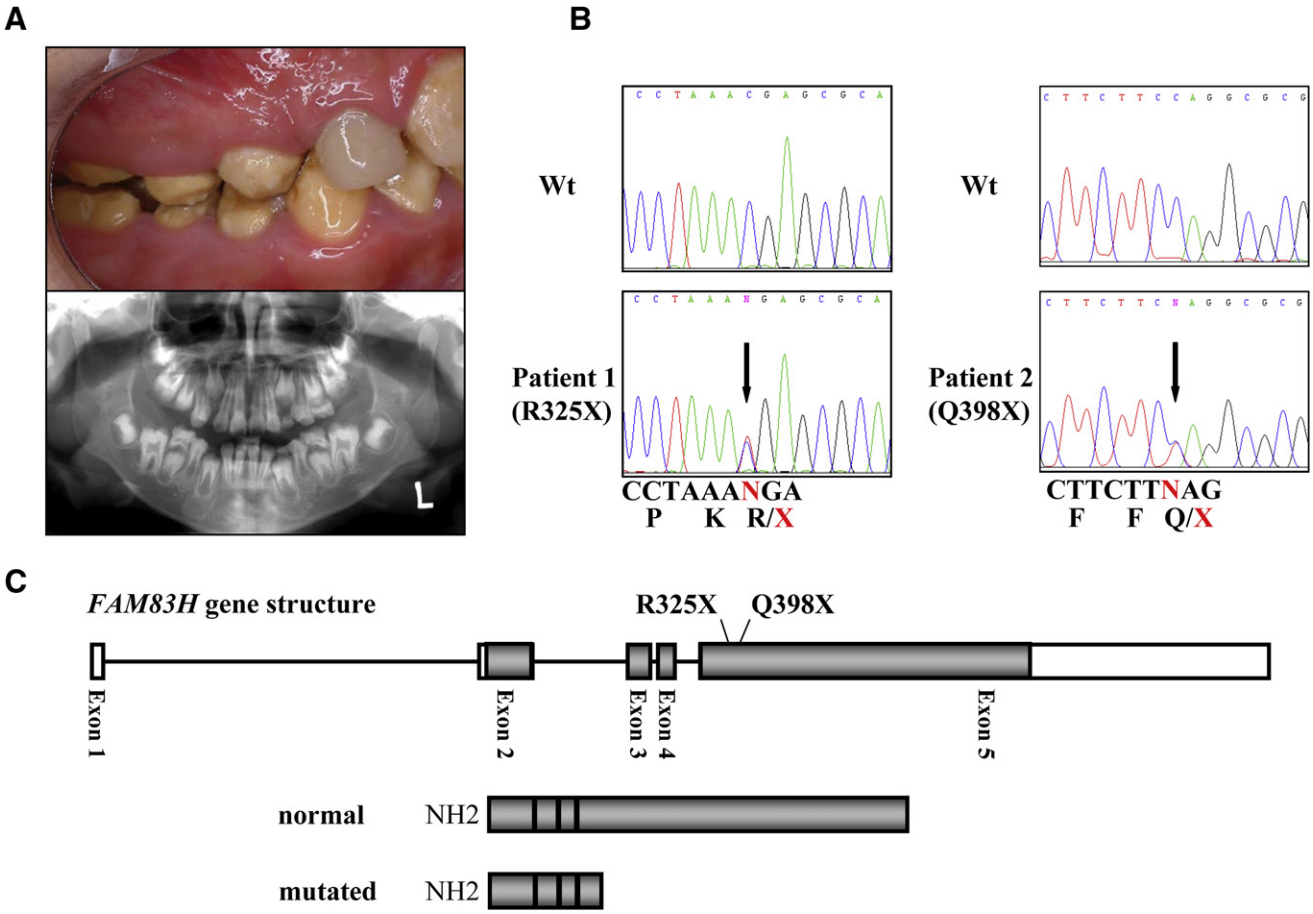

Figure 2. Mutations in *FAM83H*

(A) Clinical photograph (upper) and panoramic radiograph (lower) of an affected individual in the ADHCAI family 2.

(B) The DNA sequence of a segment of *FAM83H* exon 5 for R325X (left) and Q398X (right) mutation of patients and wild-type sequence (Wt). Nucleotide sequences and corresponding amino acids are shown below each chromatogram. The positions of nucleotide changes are marked by black arrows.

(C) Gene structure of *FAM83H*. Five exons (box) and introns (line) were drawn (upper). The number of each exon is shown below the gene structure. The position of each mutation is marked by black lines above the gene structure. Darkened boxes represent coding regions. Normal and mutated protein structure were drawn (below)

sensitivity, most of the dentitions of affected individuals were extensively restored, which precluded accurate assessment of their original condition. Several affected individuals in the first kindred (R325X) exhibited an anterior openbite, a sign that often accompanies AI regardless of type or genetic cause.

The primary structure of FAM83H gives little indication of its potential functions. The FAM83H deduced amino acid sequence was analyzed by a number of predictive algorithms. *SignalP 3.0* predicted that FAM83H is not a secreted protein. Interestingly, the *Nine Amino Acids Transactivation Domain (9aa TAD) Prediction Tool* identified DLLSEVLEA (amino acids 162–170) as a motif that is common to the transactivation domains of many transcription factors.

RT-PCR analyses of multiple tissues were positive for *FAM83H* expression; on the basis of expressed sequence tag (EST) analysis it appears to be ubiquitously expressed. FAM83H is likely to function in multiple cell types. The observation that dramatic enamel defects occur in the hemizygous condition with no apparent phenotype in other tissues suggests that developing teeth are the only organs dependent upon normal to nearly normal levels of FAM83H expression and that mutations in both alleles might produce a syndrome with enamel defects as one feature. The truncated FAM83H expressed in our two ADHCAI kindreds might have lost an important region, which interacts with an ameloblast-specific component that is critical for normal calcification of the enamel layer.

Ameloblasts progress through several functional stages to carry out the sequential processes of crystal initiation, elongation, and maturation. The growing hydroxyapatite crystals consume calcium and phosphate ions and generate hydrogen ions, so ameloblasts must constantly adjust their secretory and reabsorptive activities to maintain favorable conditions for biomineralization. Very little is understood about ameloblast differentiation, the cellular feedback mechanisms that adjust secretions according to needs, and the physiological mechanisms of ion transport

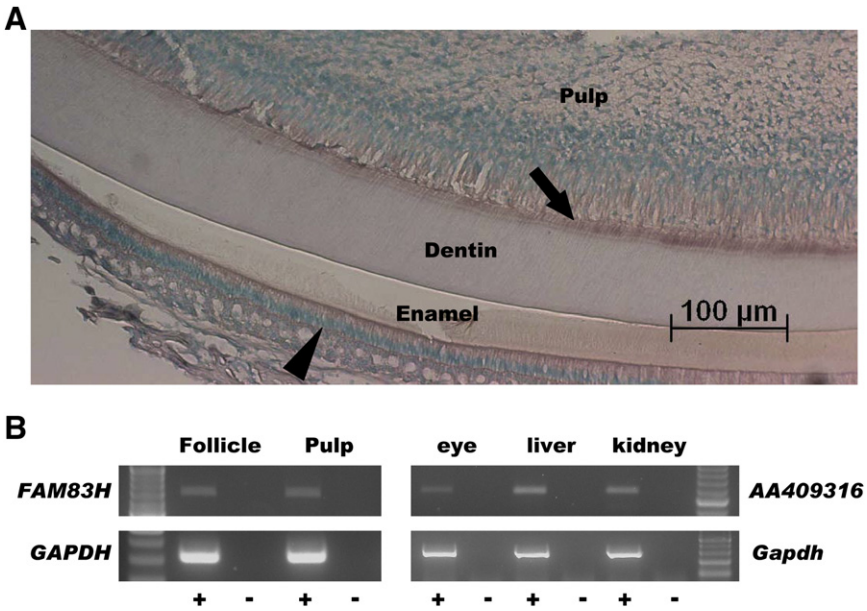

Figure 3. In Situ Hybridization and RT-PCR

(A) Expression of *AA3409316*, mouse homolog of human *FAM83H*, was detected by DIG labeled antisense RNA probe. Expression in the ameloblast (arrowhead) and odontoblast (arrow) can be seen in the anterior tooth of a 3-week-old mouse mandible.

(B) RT-PCR analysis shows that *FAM83H* is expressed in the ameloblast and odontoblast. *AA3409316* expression was detected in the mouse eye, liver, and kidney (+, reactions with reverse transcriptase; −, reactions without reverse transcriptase).

that maintain an appropriate degree of saturation for the extracellular fluid. This discovery that *FAM83H* defects cause ADHCAI will stimulate significant research into the roles that *FAM83H* plays during amelogenesis.

Acknowledgments

We thank all of the family members involved in this study for their cooperation. This work was supported by a grant from the Korea Health 21 Research and Development (R&D) Project (Ministry of Health and Welfare, Republic of Korea) (A060010) and in part by the Korea Science and Engineering Foundation (KOSEF) through the Biotechnology R&D program (2006-05229).

Received: August 29, 2007
Revised: September 25, 2007
Accepted: September 26, 2007
Published online: February 7, 2008

Web Resources

The URLs for data presented herein are as follows:

ExonPrimer, http://ihg.gsf.de/ihg/ExonPrimer.html
GenBank, http://www.ncbi.nlm.nih.gov/Genbank/
Nine Amino Acids Transactivation Domain (9aa TAD) Prediction Tool, https://emb1.bcc.univie.ac.at/toolbox/9aatad/webtool.htm
Online Mendelian Inheritance in Man (OMIM), http://www.ncbi.nlm.nih.gov/Omim/
Primer3, http://frodo.wi.mit.edu/cgi-bin/primer3/primer3_www.cgi
SignalP 3.0, http://www.cbs.dtu.dk/services/SignalP/

Accession Numbers

The GenBank accession numbers for *FAM83H* and *AA409316* reported in this paper are NM_198488 and NM_134087, respectively.

References

1. Simmer, J.P., and Fincham, A.G. (1995). Molecular mechanisms of dental enamel formation. Crit. Rev. Oral Biol. Med. *6*, 84–108.
2. Daculsi, G., and Kerebel, B. (1978). High-resolution electron microscope study of human enamel crystallites: size, shape, and growth. J. Ultrastruct. Res. *65*, 163–172.
3. Warshawsky, H., Bai, P., and Nanci, A. (1987). Analysis of crystallite shape in rat incisor enamel. Anat. Rec. *218*, 380–390.
4. Salido, E.C., Yen, P.H., Koprivnikar, K., Yu, L.C., and Shapiro, L.J. (1992). The human enamel protein gene amelogenin is expressed from both the X and the Y chromosomes. Am. J. Hum. Genet. *50*, 303–316.
5. Hu, C.C., Hart, T.C., Dupont, B.R., Chen, J.J., Sun, X., Qian, Q., Zhang, C.H., Jiang, H., Mattern, V.L., Wright, J.T., et al. (2000). Cloning human enamelin cDNA, chromosomal localization, and analysis of expression during tooth development. J. Dent. Res. *79*, 912–919.
6. Toyosawa, S., Fujiwara, T., Ooshima, T., Shintani, S., Sato, A., Ogawa, Y., Sobue, S., and Ijuhin, N. (2000). Cloning and characterization of the human ameloblastin gene. Gene *256*, 1–11.
7. Bartlett, J.D., Simmer, J.P., Xue, J., Margolis, H.C., and Moreno, E.C. (1996). Molecular cloning and mRNA tissue distribution of a novel matrix metalloproteinase isolated from porcine enamel organ. Gene *183*, 123–128.
8. Gibson, C.W., Yuan, Z.A., Hall, B., Longenecker, G., Chen, E., Thyagarajan, T., Sreenath, T., Wright, J.T., Decker, S., Piddington, R., et al. (2001). Amelogenin-deficient mice display an amelogenesis imperfecta phenotype. J. Biol. Chem. *276*, 31871–31875.
9. Seedorf, H., Klaften, M., Eke, F., Fuchs, H., Seedorf, U., and Hrabe de Angelis, M. (2007). A mutation in the enamelin gene in a mouse model. J. Dent. Res. *86*, 764–768.
10. Fukumoto, S., Kiba, T., Hall, B., Iehara, N., Nakamura, T., Longenecker, G., Krebsbach, P.H., Nanci, A., Kulkarni, A.B., and Yamada, Y. (2004). Ameloblastin is a cell adhesion molecule required for maintaining the differentiation state of ameloblasts. J. Cell Biol. *167*, 973–983.

11. Caterina, J.J., Skobe, Z., Shi, J., Ding, Y., Simmer, J.P., Birkedal-Hansen, H., and Bartlett, J.D. (2002). Enamelysin (matrix metalloproteinase 20)-deficient mice display an amelogenesis imperfecta phenotype. J. Biol. Chem. *277*, 49598–49604.
12. Kim, J.W., Simmer, J.P., Hu, Y.Y., Lin, B.P., Boyd, C., Wright, J.T., Yamada, C.J., Rayes, S.K., Feigal, R.J., and Hu, J.C. (2004). Amelogenin p.M1T and p.W4S mutations underlying hypoplastic X-linked amelogenesis imperfecta. J. Dent. Res. *83*, 378–383.
13. Kim, J.W., Seymen, F., Lin, B.P., Kiziltan, B., Gencay, K., Simmer, J.P., and Hu, J.C. (2005). ENAM mutations in autosomal-dominant amelogenesis imperfecta. J. Dent. Res. *84*, 278–282.
14. Kim, J.W., Simmer, J.P., Hart, T.C., Hart, P.S., Ramaswami, M.D., Bartlett, J.D., and Hu, J.C. (2005). MMP-20 mutation in autosomal recessive pigmented hypomaturation amelogenesis imperfecta. J. Med. Genet. *42*, 271–275.
15. Hu, J.C., Chun, Y.H., Al Hazzazzi, T., and Simmer, J.P. (2007). Enamel formation and amelogenesis imperfecta. Cells Tissues Organs *186*, 78–85.
16. Simmer, J.P., Fukae, M., Tanabe, T., Yamakoshi, Y., Uchida, T., Xue, J., Margolis, H.C., Shimizu, M., DeHart, B.C., Hu, C.C., et al. (1998). Purification, characterization, and cloning of enamel matrix serine proteinase 1. J. Dent. Res. *77*, 377–386.
17. Hart, P.S., Hart, T.C., Michalec, M.D., Ryu, O.H., Simmons, D., Hong, S., and Wright, J.T. (2004). Mutation in kallikrein 4 causes autosomal recessive hypomaturation amelogenesis imperfecta. J. Med. Genet. *41*, 545–549.
18. Kim, J.W., Simmer, J.P., Lin, B.P., Seymen, F., Bartlett, J.D., and Hu, J.C. (2006). Mutational analysis of candidate genes in 24 amelogenesis imperfecta families. Eur. J. Oral Sci. *114* (*Suppl 1*), 3–12.
19. Witkop, C.J. Jr., and Sauk, J.J. Jr. (1976). Heritable defects of enamel. In Oral Facial Genetics, R.E. Stewart and G.H. Prescott, eds. (St. Louis: C.V. Mosby Co.), pp. 151–226.
20. Witkop, C.J. Jr. (1988). Amelogenesis imperfecta, dentinogenesis imperfecta and dentin dysplasia revisited: Problems in classification. J. Oral Pathol. *17*, 547–553.
21. Bartlett, J.D., Ganss, B., Goldberg, M., Moradian-Oldak, J., Paine, M.L., Snead, M.L., Wen, X., White, S.N., and Zhou, Y.L. (2006). 3. Protein-protein interactions of the developing enamel matrix. Curr. Top. Dev. Biol. *74*, 57–115.
22. Yamakoshi, Y., Hu, J.C., Zhang, H., Iwata, T., Yamakoshi, F., and Simmer, J.P. (2006). Proteomic analysis of enamel matrix using a two-dimensional protein fractionation system. Eur. J. Oral Sci. *114* (*Suppl 1*), 266–271.
23. Fincham, A.G., Moradian-Oldak, J., and Simmer, J.P. (1999). The structural biology of the developing dental enamel matrix. J. Struct. Biol. *126*, 270–299.
24. Hu, J.C., Yamakoshi, Y., Yamakoshi, F., Krebsbach, P.H., and Simmer, J.P. (2005). Proteomics and genetics of dental enamel. Cells Tissues Organs *181*, 219–231.
25. Iwasaki, K., Bajenova, E., Somogyi-Ganss, E., Miller, M., Nguyen, V., Nourkeyhani, H., Gao, Y., Wendel, M., and Ganss, B. (2005). Amelotin—a novel secreted, ameloblast-specific protein. J. Dent. Res. *84*, 1127–1132.
26. Hart, P.S., Wright, J.T., Savage, M., Kang, G., Bensen, J.T., Gorry, M.C., and Hart, T.C. (2003). Exclusion of candidate genes in two families with autosomal dominant hypocalcified amelogenesis imperfecta. Eur. J. Oral Sci. *111*, 326–331.
27. Mendoza, G., Pemberton, T.J., Lee, K., Scarel-Caminaga, R., Mehrian-Shai, R., Gonzalez-Quevedo, C., Ninis, V., Hartiala, J., Allayee, H., Snead, M.L., et al. (2007). A new locus for autosomal dominant amelogenesis imperfecta on chromosome 8q24.3. Hum. Genet. *120*, 653–662.
28. Lindner, T.H., and Hoffmann, K. (2005). easyLINKAGE: A PERL script for easy and automated two-/multi-point linkage analyses. Bioinformatics *21*, 405–407.